Effect of Iron Ion in the Thermal Decomposition of 50 mass % Hydroxylamine/Water Solutions

Lizbeth O. Cisneros, William J. Rogers, and M. Sam Mannan*

Mary Kay O'Connor Process Safety Center, Chemical Engineering Department, Texas A&M University System, College Station, Texas 77843-3122

Xinrui Li and Hiroshi Koseki

National Research Institute of Fire and Disaster, Mitaka, Tokyo, Japan

This paper presents thermal decomposition behavior of 50 mass % hydroxylamine/water solutions (HA) when contacted with iron in the form of ferric oxide, ferrous ion, and ferric ion. If HA comes in contact with iron ion (Fe^{3+} or Fe^{2+}), even in small concentrations and at ambient temperatures, it reacts violently to produce a bubbling system with very little vapor−liquid disengagement. A great amount of energy, ∼4.0 kJ/g, is released, in a very short period of time, which results in boiling of the reaction mass. The measured heat of reaction for hydroxylamine without iron ion was 3.78 kJ/g. Rust causes heterogeneous iron catalysis of the reaction, which is not as violent as homogeneous iron catalysis, where even 0.0004 mol % (10 ppm) of iron ion added at room temperature will under adiabatic conditions trigger the complete decomposition of hydroxylamine.

1. Introduction

The thermal behavior of 50 mass% hydroxylamine/water solution (HA) decomposition alone and in the presence of some metal surfaces has been reported previously.[1−4] Nevertheless, to the best of our knowledge, the effect of iron ion on the thermal decomposition parameters, such as onset temperature, maximum temperature, maximum pressure, self-heat rates, and pressure generation rates, has never been reported. Iron ion contamination can cause uncontrollable runaway reactions that may lead to incidents. This publication presents reaction behavior of HA and iron ion carried out under adiabatic conditions. Information presented in this publication may help elucidate the root causes of recent hydroxylamine related industrial incidents.

2. Background

In 1865 Lossen discovered hydroxylamine by reducing ethyl nitrate with tin (granular) and hydrochloric acid.[5] Divers[5] divided metals into two groups depending on the products that they formed when contacted with free nitric acid: metals such as copper, mercury, silver, and bismuth, which produce nitrous acid, metal nitrate, and water, comprise the first group, and metals such as tin, zinc, cadmium, magnesium, aluminum, lead, iron, or alkali metals, which produce ammonia, comprise the second group. Some of the metals in the second group can produce hydroxylamine. This information may be useful to rationalize the thermal behavior of hydroxylamine upon contacting metals, since hydroxylamine is considered to be an intermediate in the reduction of nitric oxide[6] to ammonia:

$$NO \rightarrow NH_2OH \rightarrow NH_3 \qquad (1)$$

Thus, it can be hypothesized that metals in the second group are more likely to decompose hydroxylamine faster, although, to the best of our knowledge, information regarding reaction behavior in terms of exothermic activity, self-heat rates, or pressure generation to prove this hypothesis is not available.

There are several publications that describe possible reaction mechanisms when hydroxylamine comes in contact with metals such as tin,[5] silver(I),[7,8] manganese(III),[9] and cobalt(III).[10,11] None of these publications suggested a possible violent reaction of hydroxylamine in the presence of the metal or metal ions.

This publication presents valuable data regarding the hazard posed by the thermal decomposition of hydroxylamine free base in contact with iron ion. Onset temperatures, maximum temperature, maximum pressure, noncondensable pressure, heat rate as a function of temperature, pressure rate as a function of temperature, and time to maximum rate are among the useful contributions presented. To the best of our knowledge, none of this information has ever been reported. In fact, some references may be misleading; for example, *Chemical risk analysis. A practical handbook*[12] states that hydroxylamine does not have a dangerous reaction with transition metals, metal halides ($FeCl_3$, for example), or metal oxides, contrary to our observations.

3. Experimental Details

3.1. Samples. 3.1.1. Hydroxylamine Samples. Two sources of 50 mass % hydroxylamine/water were used in the present study: Aldrich hydroxylamine, 99.999%, 50 mass % solution in water (HA), catalog no. 46,780-4, and hydroxylamine, 50 mass % solution in water with added stabilizers, were supplied by an industrial source (HA-ind). The Aldrich hydroxylamine samples featured a nominal high purity and contained no added stabilizers. All hydroxylamine samples were used in the received condition without further analysis or purification.

10.1021/je030121p CCC: $25.00
Published on Web 07/11/2003

3.1.2. Ferric Oxide Solution. For some experiments, a suspension of ferric oxide (Fe_2O_3) was prepared using iron(III) oxide, 99.998%, from Aldrich, catalog no. 25,572-6, formula weight 159.69, 70.3% Fe concentration. The water used was Aldrich reagent grade, catalog no. 32,007-2. A dark red, 0.0029 mol % (90 ppm) suspension was prepared, since ferric oxide, or rust, is not very soluble in water.

3.1.3. Ferric Ion Solution. A 0.0029 mol % (90.8 ppm) ferric ion solution, Fe^{3+}, was made using ammonium iron(III) sulfate dodecahydrate, 99.99+% [$NH_4Fe(SO_4)_2 \cdot 12H_2O$, Aldrich catalog no. 43152-4], and Aldrich reagent grade water, catalog no. 32,007-2. The physical appearance of the solution was yellowish. The same source for the ferric ion was used in the experiments performed with the APTAC and with the flux calorimeter.

3.1.4. Ferrous Ion Solutions. A 0.004 mol % (90 ppm) ferrous ion, Fe^{2+}, solution was prepared using iron(II) sulfate hydrate, 99.999% ($FeSO_4 \cdot xH_2O$, Aldrich catalog no. 45027-8), which contains 21.4 mass % iron by titration and Aldrich reagent grade water, catalog number 32,007-2. The physical appearance of the solution was greenish. The solutions of Fe^{2+} are known to oxidize in the presence of air to Fe^{3+}, so special care was taken to use the solution as quickly as possible. During the time that the experiments were run, no visible signs of Fe^{3+} formation were observed, such that the solution remained greenish and no precipitates were formed (Fe^{3+} sulfates and hydrates are brown). Ammonium iron(II) sulfate hexahydrate ($Fe(NH_4)_2(SO_4)_2 \cdot 6H_2O$) was the ferrous ion source used in the experiments performed in the flux calorimeter.

3.2. Apparatus. Most of the data presented in this paper were collected with an automatic pressure tracking adiabatic calorimeter (APTAC) using the adiabatic mode; details of the apparatus are presented elsewhere.[13] The APTAC apparatus was modified so a small amount of liquid (approximately 1 g) could be added to the sample cell during an experiment.[14] For this purpose, a two 3.2 mm and two 1.6 mm orifice tube heater assembly was designed and fabricated. One 3.2 mm hole was used to introduce a 25 cm long metal needle to inject the iron solution (the metal needle never touched the HA contained in the sample cell because the solution was injected through the tube heater assembly approximately 1 cm above the HA level), and the other 3.2 mm tube was used to introduce a 1.6 mm diameter Teflon-coated thermocouple so the iron was the only metal in contact with the HA solution. One of the 1.6 mm tubes was used for sampling the noncondensable gaseous decomposition products at the end of the experiment, and the other one was connected to a pressure transducer. The HA heat of reaction was measured using a flux calorimeter (Setaram C 80 II). The Setaram C80 is a mixing and reaction energy calorimeter based on the Calvet heat flux principle for measuring energies of mixing and reaction from ambient to 300 °C.[15]

3.3. Analytical Methods. For the analytical measurements of the gas phase products, a 3 T Fourier transform mass spectrometer (FTMS), which is also known as an ion cyclotron resonance mass spectrometer (ICR-MS), was used. The source was electron impact (EI) at 70 eV for 5 ms with scanning ranging from 11 000 to 10 000 *m/z* (mass to charge). The sample was introduced into the FTMS chamber until a pressure of 4.0×10^{-6} Pa was achieved.

The gaseous products were also analyzed using a gas chromatograph (GC), since the possible H_2 contained in the decomposition products cannot be detected in the EI-FTMS. The chromatograph was a Varian 3400 with a thermal conductivity detector (TCD) and a flame ionization detector (FID). The sample size was 0.5 mL for the TCD side and 0.25 mL for the FID side. A Chromsorb 107 column (3.66 m × 3.2 mm, 80/100) and a 13X molecular sieve column (1.83 m × 3.2 mm, 40/60) were used on the TCD side. An alumina plot capillary column (40 m × 0.53 mm × 15 μm) was used on the FID side. Four switching valves were used to facilitate sampling and column selection. The temperature program used was as follows: 4 min at 35 °C, then a 10 °C/min ramp until 200 °C, and finally 20 min at 200 °C. Actually, only the TCD detector was useful for the particular gas mixture, since no peaks were detected by the FID.

Liquid products were analyzed for ammonia and water. The ammonia quantification method consisted of adding MgO to the ammonia-containing sample and titrating the resulting mixture with NaOH with methyl red as an indicator.[16] The water content of the liquid residue was analyzed using a Karl Fischer moisture method.[17]

3.4. Experimental Method. 3.4.1. APTAC Experiments. Experimental runs were performed in spherical sample cells of 130 cm^3 nominal volume and of borosilicate glass. It was presumed that glass cells provided a neutral environment without significant catalysis for the HA decomposition reaction. HA samples were transferred to sample cells using disposable plastic pipets. Sample masses were obtained by weight differences. Because of the relatively small amounts of sample, no stirring was used during the APTAC runs. A sample thermocouple with a Teflon-coated sheath was used to prevent the metal surface from contacting the sample.

The APTAC experiments reported here were performed in a closed cell environment with air above the sample. The heating mode was heat−wait−search, in which the sample was heated to an initial search temperature of 30 °C and the temperature was allowed to stabilize (20 min). Once the searching period had begun, the injection valve was manually opened and the iron solution (1 mL) was introduced by a precision syringe connected to a long needle which dropped the iron solution ≈1 cm above the HA sample. Then if exothermic activity was detected, as exhibited by a threshold temperature rise of 0.1 °C/min, the apparatus followed the reaction adiabatically until the reaction ended or until one of the preselected safety shutdown criteria was met (shutdown criteria: temperature, 460 °C; pressure, 10 300 kPa; temperature rate, 400 °C/min; pressure rate, ≈68 900 kPa/min). If no exothermic activity was detected within 20 min, the sample was heated to the next search temperature (10 °C higher), and the procedure was repeated until a preset maximum search temperature was attained (200 °C).

3.4.2. Flux Calorimeter Experiments. For the experiments reported in this work, 0.2 g of HA-ind was placed in the sample vessel and 0.2 g of α-alumina was placed in the reference vessel. For some experiments the HA-ind was mixed with ≈0.05 g of 0.0022 mol % (50 ppm) ferrous or ferric ion solution immediately before placing the sample container in the flux calorimeter. The scanning rate was 0.1 °C/min from (25 to 300) °C.

3.5. Uncertainties. A type N thermocouple was used to measure sample temperatures with an overall absolute uncertainty of ≈±1 °C, and it was checked periodically at 0 °C using an ice bath. Sample pressures were measured with Sensotec absolute pressure transducers with an overall uncertainty of ≈±42 kPa and were checked frequently for agreement with ambient pressures. Sample masses were measured with a precision of ±0.01 g.

Table 1. Summary of Visualization Experiments

experiment	observation
5 mL of HA + 1 mL of 1800 ppm Fe_2O_3	no apparent reaction
5 mL of HA + 1 mL of 1622 ppm Fe^{2+}	very violent reaction with boiling of the reacting mixture; brown precipitate formed
5 mL of HA + 1 mL of 8991 ppm Fe^{3+}	very violent reaction with boiling of the reacting mixture; brown precipitate formed
5 mL of NH_4OH + 1 mL of 8991 ppm Fe^{3+}	no violent reaction, only change in color due to formation of brown precipitate
liquid residue of HA + 1 mL of 8991 ppm Fe^{3+}	no violent reaction, only change in color due to formation of brown precipitate
1 mL of NH_4OH + 1 mL of HA	no indication of a reaction

Table 2. HA Decomposition in the Presence of Ferric Oxide Data Summary[a]

identification	$[Fe_2O_3]$ ppm	initial[b] wt g ± 0.01	final wt g ± 0.01	liquid residue	solid residue
Fe_2O_3, 10	10.0	9.03	6.33	slightly green	white fluffy
Fe_2O_3, 200	199.7	9.01	6.80	slightly blue	white fluffy

[a] $\phi = 2$. [b] Initial HA sample plus 1 mL of Fe_2O_3 solution.

To measure the uncertainty for the iron solution addition, a water injection was made in exactly the same way as the iron solution injections. The injected mass was 0.99 g, which is equal to the target value (1 g) within the balance uncertainty (±0.01 g).

4. Results and Discussion

Due to the lack of knowledge of the behavior of hydroxylamine in the presence of ferrous or ferric ion, a minor incident occurred in the laboratory during the first ferrous ion experiment. A sample of 8 g of HA was placed in a cell, and 1 mL of a 0.52 mol % (16 000 ppm) Fe^{2+} solution (from iron(II) sulfate hydrate) was added. A brown precipitate formed and, immediately after that, a violent reaction that created a bubbling system with very little vapor−liquid disengagement took place. At the end of the reaction the sample cell was practically empty and the hot reaction mass was dispersed as far as 2 m. Under these particular conditions the cell remained intact, but a ruptured cell could result from a higher concentration of iron ion, which will increase the pressure generation rate, or a closed cell experiment, since the pressure generated inside the sample cell will create a huge pressure differential across the sample cell wall which most probably will lead to the mechanical failure of the glass sample cell. The dark brown or blackish precipitate is characteristic of Fe^{3+} compounds and can be either ferric oxide (Fe_2O_3) or iron hydroxide FeO(OH). Either way, the reaction involved the oxidation of Fe^{2+} to Fe^{3+}, and because the brown color was present a few seconds before the reaction became violent, this iron oxidation may be the first step in the reaction.

A similar experiment to the one described above was repeated inside a fume hood under controlled conditions, so this violent reaction could be recorded by a digital camera. To slow the reaction, the final HA/iron(II) solution contained only 0.0087 mol % (197 ppm) Fe^{2+}. Frames of that video recording can be found in ref 14. The video recording showed that the reaction starts with the production of a brown precipitate at the surface of the HA solution while the content in the bottom part of the beaker is not reacting yet. The reaction front moves quickly down the beaker, releasing heat, evaporating the solvent, and producing colorless gases. The violence of the reaction can be appreciated from the production of bubbles that rise from the bottom to the top part of the beaker, where the reaction mixture is exiting the beaker. The reaction stops only when all the HA has been consumed and only a small amount of precipitate remains in the beaker.

Some experiments where the reactants were premixed and then tested with the APTAC resulted in poor reproducibility and are not included in this article. An important qualitative observation from these preliminary experiments was the clearly marked presence of two maxima in both the heat rate and pressure rate data. These two peaks can be attributed to two different reactions, the first one forming the precipitate. After these experiments it became clear that, to obtain accurate measurements of the thermal decomposition of HA when in contact with iron ion, the injection of the latter should be made once the apparatus has begun to record data.

Table 1 presents a summary of some visual experiments performed. These experiments are useful to test for violent reactions, color of precipitate, and gas evolution. As can be seen from Table 1, it seems that the same precipitate is obtained when mixing Fe^{3+} with ammonia or hydroxylamine, although the reaction with ammonia is not violent. Some Fe^{3+} was used to test for possible unreacted hydroxylamine remaining in the liquid residue after a thermally induced HA runaway reaction, but no traces of hydroxylamine were detected, since there was no apparent violent reaction. Mixing HA with ammonia does not generate any apparent reaction. The difference of HA reactivity toward homogeneous (ion in solution) and heterogeneous (metal surface in suspension) catalysis is clearly seen in the visualization experiments of Table 1, since mixing HA with a suspension of ferric oxide (Fe_2O_3 is not soluble in water) does not generate any apparent reaction, in contrast to the experiment between HA and ferrous or ferric ion, where a very violent reaction is observed. As shown in the table, mixing HA with ferrous or ferric ion will produce similar results.

4.1. Ferric Oxide Experiments. It was important to test the catalytic effect of rust (ferric oxide, Fe_2O_3), since it is a common industrial contaminant. Table 2 presents a summary of the APTAC experiments with ferric oxide. It is important to note that rust is not very soluble in water, so its catalytic effect is not expected to be very significant. Open literature information was used to suggest an identity for the white residue.[18] Given the species involved in the reaction, a possible identity for the precipitate is iron(II) hydroxide [$Fe(OH)_2$].

Table 3 presents a summary of the measured parameters for the decomposition of HA in the presence of 0.0004 mol % and 0.0088 mol % (10 and 200 ppm) iron oxide. As can be seen from this table, the onset temperature decreased by 9 °C when the iron oxide concentration increased 20 times. The time to the maximum rate was reduced signifi-

Table 3. HA Decomposition in the Presence of Ferric Oxide Decomposition Parameters[a]

	θ_{on}	θ_{max}	$\Delta\theta_{adb}$	P_{max}	noncondensables	t_{MR}
sample	°C	°C	°C	kPa	kPa	min
Fe_2O_3, 10	111	284	173	8749	751	223
Fe_2O_3, 200	102	279	176	8184	751	51

[a] $\phi = 2$.

Table 4. HA Decomposition in the Presence of Iron Ion Data Summary

identification	[Fe ion] ppm	initial[a] wt g ± 0.01	final wt g ± 0.01	liquid residue	solid residue
Fe^{3+}, 1	10.1	9.03	7.50	slightly blue	brown
Fe^{3+}, 2	10.0	9.10	7.53	blue	brown
Fe^{3+}, 3	10.1	9.03	7.52	blue	brown
Fe^{3+}, 4	10.0	9.05	7.45	blue	brown
Fe^{3+}, 5	10.1	9.03	7.46	blue	brown
Fe^{2+}, 1	10.0	9.02	7.25	blue	brown
Fe^{2+}, 2	10.0	9.01	7.32	blue	brown
Fe^{2+}, 3	10.8	9.01	7.44	blue	brown
Fe^{2+}, 4	9.9	9.06	7.42	slightly blue	brown
Fe^{2+}, 5	9.9	9.08	7.46	blue	brown

[a] Initial HA sample plus 1 mL of the respective iron ion solution.

cantly (around 4.7 times) for the sample with the highest concentration of catalyst. As expected, only the dynamic parameters θ_{on}, θ_{max}, P_{max}, and t_{MR} (those that depend on the self-heating rate) were affected by the amount of contaminant. The static parameters $\Delta\theta_{adb}$ and noncondensable pressure remained unchanged.

4.2. Ferric and Ferrous Ion Experiments. It was hypothesized that the ions in solution produce a more violent reaction than the heterogeneous iron reaction (Fe_2O_3) due to higher ion availability. To test for a difference in the reaction due to the oxidation state of iron, Fe^{3+} and Fe^{2+} solutions were prepared. Table 4 presents a summary of the experiments performed using ferric and ferrous ion solutions.

The blue residue is explained by copper contamination from the tube heater assembly, since an analysis for one of the samples (Fe^{3+}, 5) revealed 100 ppm of copper. It seems that the same precipitate is formed irrespective of the initial oxidation state of the iron ion. Iron hydroxide [FeO(OH)] or rust [Fe_2O_3] is a possible identity for this precipitate. Table 5 presents the decomposition parameters measured for the HA decomposition when in contact with ferrous and ferric ions. It can be seen that the decomposition behavior was the same within the experimental error irrespective of the initial oxidation state of the ion for all the reported parameters. It is important to note that the reaction started immediately after the injection of the ion solution. Although only 0.0004 mol % (10 ppm) Fe^{2+} or Fe^{3+} was used, the dramatic effect of the contaminant can be appreciated from Figure 1. The vertical line in the plot represents the injection point, where the time has been

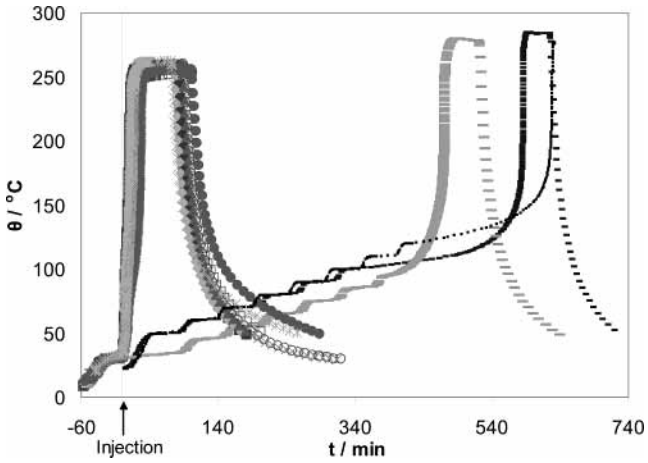

Figure 1. Temperature vs corrected time for HA decomposition in the presence of iron ion: −, Fe_2O_3, 10 ppm; —, Fe_2O_3, 200 ppm; □, Fe^{3+}, 1; ◇, F^{3+}, 2; △, Fe^{3+}, 3; ○, Fe^{3+}, 4; ×, Fe^{3+}, 5; ■, Fe^{2+}, 1; ◆, Fe^{2+}, 2; ▲, Fe^{2+}, 3; ●, Fe^{2+}, 4; ∗, Fe^{2+}, 5; -, HA.

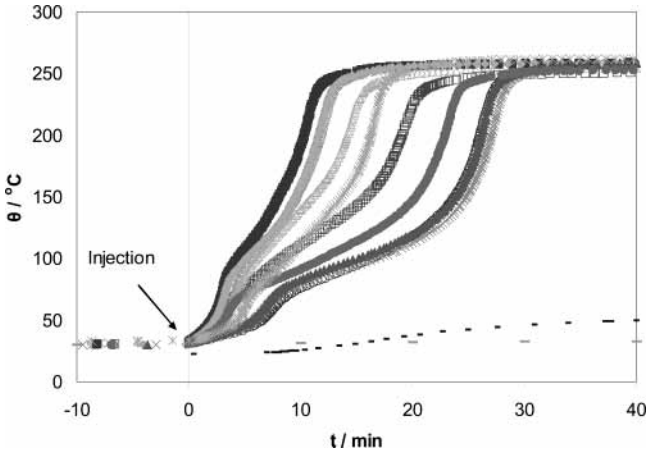

Figure 2. Temperature vs corrected time for HA decomposition in the presence of iron ion for 40 min following injection: −, Fe_2O_3, 10 ppm; —, Fe_2O_3, 200 ppm; □, Fe^{3+}, 1; ◇, F^{3+}, 2; △, Fe^{3+}, 3; ○, Fe^{3+}, 4; ×, Fe^{3+}, 5; ■, Fe^{2+}, 1; ◆, Fe^{2+}, 2; ▲, Fe^{2+}, 3; ●, Fe^{2+}, 4; ∗, Fe^{2+}, 5; -, HA.

normalized so time = 0 represents the injection time. For comparison, the plot also includes the experiments run with ferric oxide and without any contaminant (HA). Figure 2 also presents the temperature versus time plot, but the time scale has been modified to show the initial 40 min after injection. It can be seen that there is no difference between experiments run with ferric and ferrous ion and that the reaction starts immediately after injection.

As shown in Figure 3, the pressure data follow the temperature data for the decomposition of HA with iron ion. The higher pressure acquired by the Fe_2O_3 experiments is due to vapor pressure at higher temperature, since all experiments presented in this plot have a very similar noncondensable pressure.

The presence of two well defined exothermic behaviors is clearly shown in the heat and pressure rates of Figures

Table 5. HA Decomposition Parameters in the Presence of Iron Ion

ion	runs	θ_{on}/°C	θ_{max}/°C	$\Delta\theta_{adb}$/°C	P_{max}/kPa	noncondensable/kPa
Fe^{3+}	5	immediate[a]	257 ± 3	227 ± 3	6557 ± 200	724 ± 14
Fe^{2+}	5	immediate[a]	260 ± 2	230 ± 2	6688 ± 165	710 ± 14

[a] Onset of the reaction was observed a few seconds after addition of the ion solution.

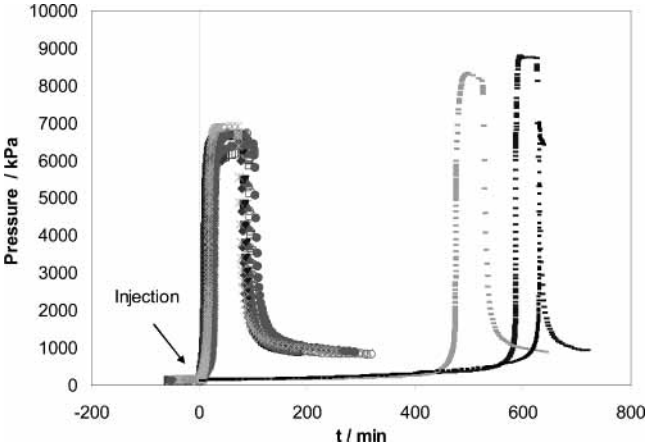

Figure 3. Pressure vs corrected time for HA decomposition in the presence of iron ion: −, Fe_2O_3, 10 ppm; —, Fe_2O_3, 200 ppm; □, Fe^{3+}, 1; ◇, F^{3+}, 2; △, Fe^{3+}, 3; ○, Fe^{3+}, 4; ×, Fe^{3+}, 5; ■, Fe^{2+}, 1; ◆, Fe^{2+}, 2; ▲, Fe^{2+}, 3; ●, Fe^{2+}, 4; ∗, Fe^{2+}, 5; -, HA.

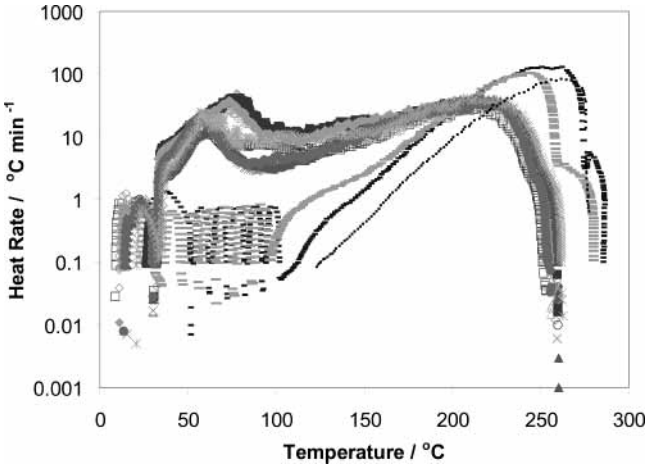

Figure 4. Heat rate plot for HA decomposition in the presence of iron ion: −, Fe_2O_3, 10 ppm; —, Fe_2O_3, 200 ppm; □, Fe^{3+}, 1; ◇, F^{3+}, 2; △, Fe^{3+}, 3; ○, Fe^{3+}, 4; ×, Fe^{3+}, 5; ■, Fe^{2+}, 1; ◆, Fe^{2+}, 2; ▲, Fe^{2+}, 3; ●, Fe^{2+}, 4; ∗, Fe^{2+}, 5; -, HA.

4 and 5, respectively. The good data reproducibility is also presented in these plots. The initial injection of the iron ion triggers the first reaction, which liberates enough thermal energy to heat the reaction mixture to the onset temperature of the second exotherm. A summary of some important parameters deduced from Figures 4 and 5 is presented in Table 6.

4.3. Flux Calorimeter Experiments. Flux calorimetry experiments were performed in collaboration with the National Research Institute for Fire and Disaster in Tokyo, Japan, to measure the heat released when HA comes in contact with ferric or ferrous ion. It is important to note that the flux calorimeter used was not modified to support an injection during an experiment, so the HA and the ion solution had to be mixed immediately before starting the experiment and, in doing so, part of the heat generated was not measured by the apparatus. Another drawback of these experiments is that, since the reaction begins immediately after mixing the HA and the ion solution, there was no opportunity to obtain a baseline. As a result, the heat flux integration was more difficult and included higher uncertainty. Figure 6 and Table 7 present the determined values. As seen in Figure 6 and Table 7, all of the

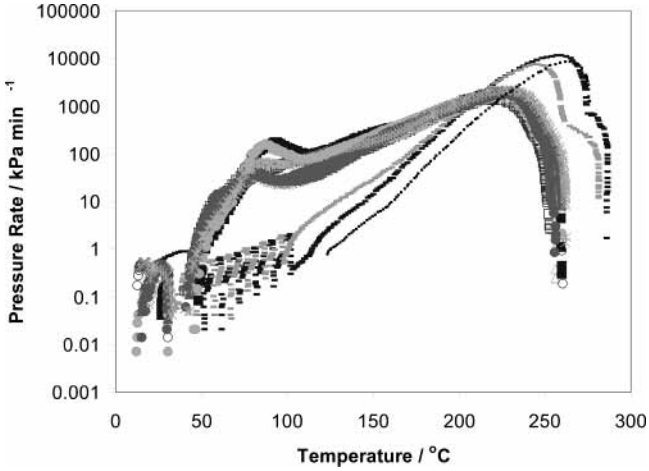

Figure 5. Pressure rate plot for HA decomposition in the presence of iron ion: −, Fe_2O_3, 10 ppm; —, Fe_2O_3, 200 ppm; □, Fe^{3+}, 1; ◇, F^{3+}, 2; △, Fe^{3+}, 3; ○, Fe^{3+}, 4; ×, Fe^{3+}, 5; ■, Fe^{2+}, 1; ◆, Fe^{2+}, 2; ▲, Fe^{2+}, 3; ●, Fe^{2+}, 4; ∗, Fe^{2+}, 5; -, HA.

Table 6. Heat and Pressure Rates for HA Decomposition in the Presence of Iron Ion

ion	replicas	ϕ	$(d\theta/dt_{max})^{1a}$ °C min^{-1}	$(d\theta/dt_{max})^2$ °C min^{-1}	$(dP/dt_{max})^1$ kPa min^{-1}	$(dP/dt_{max})^2$ kPa min^{-1}
Fe^{3+}	5	2	24 ± 16	35 ± 3	83 ± 62	1738 ± 228
Fe^{2+}	5	2	27 ± 12	38 ± 3	110 ± 90	1972 ± 165

[a] Superscripts 1 and 2 correspond to the first and second exotherms.

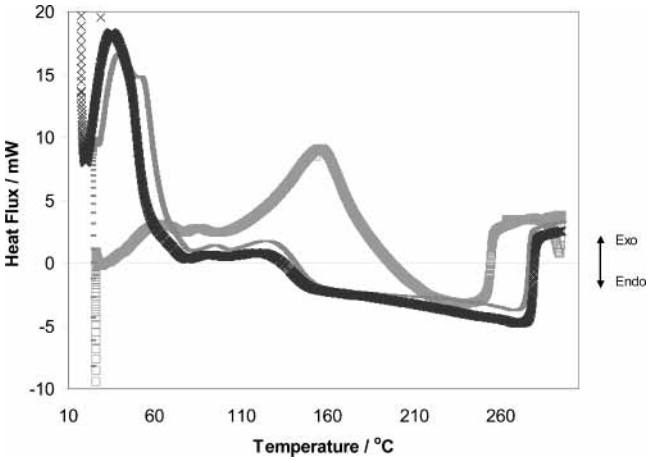

Figure 6. Heat flux for HA decomposition alone and in the presence of iron ions: □, HA; —, HA + 10 ppm Fe^{3+}; ×, HA + 10 ppm Fe^{2+}.

Table 7. Estimated Heat of Reaction for the HA Decomposition in the Presence of Iron Ions

sample	$-\Delta H_{rxn}$/(kJ g^{-1})	peak 1 %	peak 2 %	peak 3 %
HA	3.78	15.5	9.3	75.2
HA + Fe^{3+}	3.53	79.2	8.3	12.5
HA + Fe^{2+}	3.99	83.8	7.2	9.0

decomposition reactions feature three heat flow peaks, which represent three reactions. For the HA decomposition the main exothermic reaction is the third one, which exhibits an onset temperature around 110 °C, in agreement with APTAC experiments.[4] The hydroxylamine heat of

Table 8. Gas Phase Analytical Results for HA Decomposition in the Presence of Iron Ions

sample	replicas	NH_3 mol %	H_2O mol %	N_2 mol %	NO mol %	O_2 mol %	N_2O mol %	H_2 mol %
HA + Fe_2O_3	1	0.6	0	66.5	3.0	0.3	27	2.6
HA + Fe^{3+}	2	2.1 ± 0.3	0.2 ± 0.3	44.8 ± 1.4	5.9 ± 0.1	0.5 ± 0.1	46.2 ± 1.5	0.3 ± 0.1
HA + Fe^{2+}	2	1.7 ± 0.4	0.3 ± 0.3	45.6 ± 0.4	5.4 ± 0.1	0.5 ± 0.2	46.1 ± 1	0.4 ± 0.1

Table 9. Liquid Phase Analytical Results for HA Decomposition in the Presence of Iron Ions

sample	replicas	ammonia mass %	water mass %	unaccounted mass %
HA + Fe_2O_3	1	6.8	90.7	2.5
HA + Fe^{3+}	2	8.2 ± 0.5	90.2 ± 0.8	1.6 ± 1.1
HA + Fe^{2+}	2	5.1 ± 3.7	94.0 ± 4.4	0.9 ± 0.6

reaction measured was 3.78 kJ/g, which is consistent with the 3.55 kJ/g reported in ref 4. For the ferric and ferrous ion, the greater heat flux corresponds to the first reaction, which started before the flux calorimeter began collecting data. Although the total amount of heat released is similar for all three reactions, it should be noted that for the ferric and ferrous ion experiments part of the heat released was not measured and calculation of the heat released is difficult due to the lack of a baseline.

4.4. Analytical Results. Table 8 presents a summary of the composition of noncondensable gas products collected after the thermal decomposition of HA in the presence of iron. It is interesting to note that the presence of ions affected the composition of the gas mixture, except for the experiments with ferric oxide. Without the iron ions, the gas phase was roughly (70 to 30) mol % N_2/N_2O[14] compared with the approximately (50 to 50) mol % N_2/N_2O reported in Table 8. The gas phase is also more diversified with O_2, NH_3, and water, aside from the N_2, NO, N_2O, and H_2 for the HA decomposition without the iron ions.[14] As shown in Table 9, analysis of the liquid phase yielded ≈7 mass % ammonia and ≈92 mass % water.

5. Conclusions

If HA comes in contact with iron ion (Fe^{3+} or Fe^{2+}), even in concentrations as small as 0.0087 mol % (197 ppm) and at ambient temperatures, it will react violently, producing a bubbling system with very little vapor−liquid disengagement. A great amount of energy, ≈3.99 kJ/g, will be released, in a very short period of time, which will result in boiling of the reaction mass. Rust will cause heterogeneous catalysis of the reaction, which is not as violent as iron homogeneous catalysis, where even 0.0004 mol % (10 ppm) of iron ion added at room temperature will produce enough energy to trigger the complete decomposition of hydroxylamine if the system is kept adiabatic.

Homogeneous catalysis of HA takes place in two well defined exothermic reactions, the first being more aggressive than the second. The HA decomposition product distribution is affected by iron ion presence with an increase in the relative amount of N_2O produced.

Acknowledgment

The authors would like to acknowledge Mr. Xianchun Wu for his help during the analytical part of this work and Mr. Michiko Momota and Dr. Yusaku Iwata for their collaboration in this work.

Literature Cited

(1) Surjono, H.; Xiao, Z.; Sundareswaran, P. C. Understanding Thermal Stability of Hydroxylamine Freebase. Proc. 218th ACS National Meeting, New Orleans, LA, 1999.
(2) Cisneros, L. O.; Rogers, W. J.; Mannan, M. S. Adiabatic Calorimetric Decomposition Studies of 50 wt % Hydroxylamine/Water. *J. Hazard. Mater.* **2001**, *82*, 13−24.
(3) Cisneros, L. O.; Rogers, W. J.; Mannan, M. S. Thermal Decomposition Study of Hydroxylamine. Proc. 3rd Annual Mary Kay O'Connor Process Safety Center Symposium−Beyond Regulatory Compliance: Making Safety Second Nature, College Station, TX, 2000; pp 140−168.
(4) Cisneros, L. O.; Rogers, W. J.; Mannan, M. S. Effect of Air in the Thermal Decomposition of 50 Mass% Hydroxylamine/Water. *J. Hazard. Mater.* **2002**, *95* (1−2), 3−25.
(5) Divers, E. On the Production of Hydroxylamine from Nitric Acid. *J. Am. Chem. Soc.* **1883**, *43*, 443−466.
(6) Mellor, J. C. Hydroxylamine. *Compr. Treatise Inorg. Theor. Chem.* **1928**, *8*, 279−304.
(7) James, T. H. Effect of Catalyst Upon the Oxidation Products of Hydroxylamine. *J. Am. Chem. Soc.* **1942**, *64* (4), 731−734.
(8) Honig, D. S.; Kustin, K. Kinetics of the Oxidation of Some Hydroxylamines by Silver II. *Inorg. Chem.* **1972**, *11* (8), 1895−1901.
(9) Davies, G.; Kustin, K. The Stoichiometry and Kinetics of Manganese (III) Reactions with Hydroxylamine, O-methylhydroxylamine, and Nitrous Acid in Acid Perchlorate Solution. *Inorg. Chem.* **1969**, *8* (3), 484−490.
(10) Sramkova, B.; Zyka, J.; Dolezal, J. The Study of the Oxidation Properties of Cobalt (III). Part I, the Reaction of Cobalt (III) with Hydroxylamine. *J. Electroanal. Chem.* **1971**, *30*, 169−175.
(11) Sramkova, B.; Sramek, J.; Zyka, J. The Oxidation of Hydroxylamine with Cobalt (III) a Study of Variable Reaction Stoichiometry. *Anal. Chim. Acta* **1972**, *62*, 113−124.
(12) Martel, B. *Chemical Risk Analysis: A Practical Handbook*; Penton Press: London, 2000.
(13) Chippett, S.; Ralbovsky, P.; Granville, R. The APTAC: a High Pressure, Low Thermal Inertia, Adiabatic Calorimeter. Proc. Int. Symp. Runaway React., Pressure Relief Des. *Effluent Handling* **1998**, 81−108.
(14) Cisneros, L. O. Adiabatic Calorimetric Studies of Hydroxylamine Compounds. Ph.D. Chemical Engineering Dissertation, Texas A&M University, August 2002.
(15) Marliacy, P.; Courdet, J. B.; Schuffenecker, L.; Solimando, R. Dissolution Enthalpy of Anhydrous Sodium Sulfate in Water. Experimental Measurements and Treatment with the Electrolyte-NRTL Model. *J. Chem. Thermodyn.* **2002**, *34*, 579−591.
(16) *Official Methods of Analysis of AOAC International*, 17th ed.; Horowitz, W., Ed.; Method number 920.03.
(17) *Official Methods of Analysis of AOAC International*, 17th ed.; Horowitz, W., Ed.; Method number 966.20.
(18) Lide, D. R. *CRC Handbook of Chemistry and Physics*, 75th ed.; CRC Press: Boca Raton, FL, 1995; pp 4−64.

Received for review January 6, 2003. Accepted June 3, 2003. This research was sponsored by the Mary Kay O'Connor Process Safety Center, Chemical Engineering Department, Texas A&M University.

JE030121P